Eur. Phys. J. E **4**, 121–127 (2001)

THE EUROPEAN PHYSICAL JOURNAL E

EDP Sciences

Why is nacre strong? Elastic theory and fracture mechanics for biocomposites with stratified structures

K. Okumura[1,2,a] and P.-G. de Gennes[1]

[1] Physique de la Matière Condensée, Collège de France, 11, place Marcelin-Berthelot, 75231 Paris cedex 05, France
[2] Theoretical Studies, Institute for Molecular Science, Okazaki, Aichi 444-8585, Japan

Received 18 March 2000

Abstract. Nacre, stratified ceramic layers surrounded by organic matrix, is a tough material found inside certain seashells. We construct a coarse-grained elastic energy for such an anisotropic system and present an analytic solution for a notch crack normal to the stratified sheets. This analysis proves the reduction in stress concentration which was announced in our earlier work (P. G. de Gennes and K. Okumura, C. R. Acad. Sci. Paris **1**, Ser. IV, 257 (2000)) and the related increase in toughness.

PACS. 87.68.+z Biomaterials and biological interfaces – 46.50.+a Fracture mechanics, fatigue and cracks – 83.70.Dk Composite solids

1 Introduction

A number of natural materials derive their strength from a composite structure. Timber and abalone are typical examples. The former is composed of cellulose fibers in soft lignin while the latter possesses a layered structure of brittle ceramic and soft organic matrix. These composite structures (fibers and layers) appear in biomimetic materials [1–4]. Automobile tires nowadays, for example, employ laminated sheets made of fiber composites.

In this article, we propose a simple view on one of the laminated structures found in nature, *i.e.* nacre. Certain seashells like abalones contain an inner coverage of nacre. The nacre displays a high fracture toughness (comparable to those of some high-technology structural ceramics) [5–7]. The unique nacre structure is composed of alternating (nanometer-scale) layers of thin peptide matrices and $CaCO_3$ (aragonite) platelets, where 95 volume % of the composite is the inorganic material (see Fig. 1).

Several toughening mechanisms of the nacre have been examined in the literature and exploited to produce strong materials [7,2,8]: 1) crack blunting/branching, 2) microcrack formation, 3) internal stresses, etc. All these effects may be significant. Our aim here is limited; we concentrate on one possible reason —weakened tip-stress concentration, which is clearly an important factor.

For later convenience, some scales are introduced here; the thicknesses of hard inorganic layer and that of the soft organic layer are denoted $d_{\rm h}$ and $d_{\rm s}$, respectively. The

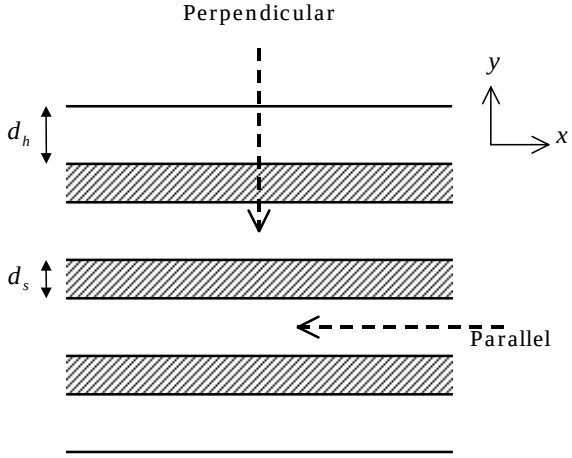

Fig. 1. Nacre structure: the (inorganic) hard-layer thickness $d_{\rm h}$ is of order of micrometer while the soft-layer (organic) thickness $d_{\rm s}$ of nanometer. The y axis is perpendicular to layers and the sample is long in the z direction. The cracks in the (y,z)-plane and in the (x,z)-plane are called the perpendicular and the parallel fractures, respectively.

Young modulus of the hard and soft layers are denoted $E_{\rm h}$ and $E_{\rm s}$, respectively, and we put

$$E_{\rm s} = \varepsilon E_{\rm h},$$

where ε is very small, and is probably around 1/5000 ($E_{\rm h}$ is about 50 GPa , while $E_{\rm s}$ may be estimated as the value of polymeric rubber, *i.e.* 1 MPa). In the following, we concentrate on one configuration, *i.e.* perpendicular fracture (see Fig. 1) under the plane strain condition, *i.e.* $e_{zx} = e_{zy} = e_{zz} = 0$. Here, e_{ij} is the strain derived from

[a] *Permanent address*: Department of Physics, Faculty of Science, Ochanomizu University, 2-1-1, Otsuka, Bunkyo-ku, Tokyo 112-8610, Japan.
e-mail: okumura@phys.ocha.ac.jp

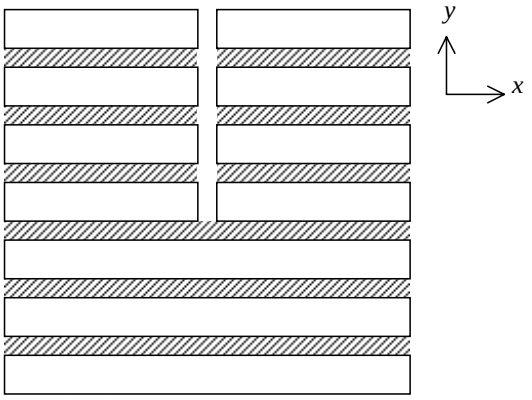

Fig. 2. Perpendicular crack in the small ε limit. The crack is abruptly ended at a soft layer; no stress concentration at the tip is expected.

the displacement field u_i, *i.e.*

$$e_{ij} = \frac{1}{2}\left(\frac{\partial u_i}{\partial x_j} + \frac{\partial u_j}{\partial x_i}\right),$$

where $(x_1, x_2, x_3) \equiv (x, y, z)$. Experimentally, it is suggested that the fracture toughness is significantly enhanced mainly in the perpendicular fracture; the perpendicular case is relevant when the sheets are bent macroscopically [5,6].

In such a layered system the stress concentration at the crack tip is weaker than in usual isotropic elastic materials [9]. This can be understood when a limiting case is considered; suppose that ε is infinitely small and the soft layer acts merely as a lubricant. In this case (as shown in Fig. 2), the fracture profile stays flat and the fracture is abruptly stopped at one thin layer; there is no stress enhancement at the tip and the fracture advances only when the remote stress σ_∞ is comparable to the intrinsic yield stress of the aragonite, which can be estimated as [10–13]

$$\sigma_{\rm YS} \simeq \sqrt{\frac{E_{\rm h}\gamma_{\rm h}}{a_{\rm h}}}, \tag{1}$$

where $a_{\rm h}$ is the typical size of a Griffith cavity in pure aragonite, and is small for the well-crystallized aragonite of nacre. Here, $\gamma_{\rm h}$ is the surface energy of pure aragonite, roughly corresponding to the energy (per area) required to breaking chemical bonds.

In the following, we try to translate this physical idea into an analytical theory; we propose a coarse-grained elastic energy for the anisotropic material and analyze the fracture profile in the perpendicular case.

The ensuing analysis is based on three conditions,

$$\begin{aligned} \varepsilon &\ll 1, \\ d_{\rm s} &\ll d_{\rm h}, \\ \epsilon &= \varepsilon d/d_s \ll 1, \end{aligned}$$

where, $d = d_{\rm s} + d_{\rm h} \simeq d_{\rm h}$.

2 Elastic energy for nacre in the thin layer limit

On the microscopic level, the Young modulus E and the Poisson ratio ν are dependent on y in our anisotropic and inhomogeneous system; the stress must be continuous but the strain field is not continuous. Thus, it is necessary to distinguish the strains in the soft and hard parts; *i.e.* $e_{ij}^{(\rm s)}$ and $e_{ij}^{(\rm h)}$. However, assuming that the thickness of layers is thin (in the sense that we can neglect the stress change over a few layers), we can introduce *a coarse-grained strain field* with the following elastic energy (see appendix):

$$f = \frac{E}{2(1-\nu^2)}e_{xx}^2 + \frac{E_0}{2}e_{yy}^2 + \frac{E_0}{1+\nu}e_{xy}^2 + \frac{\nu E_0}{1-\nu}e_{xx}e_{yy}, \tag{2}$$

where

$$\begin{aligned} E &= E_{\rm h}, \\ E_0 &= \epsilon E_{\rm h}. \end{aligned}$$

We have assumed for simplicity that the Poisson ratio is the same for both layers. As we shall see below, the size ξ of the region of stress concentration is large when compared to the repeat period: the coarse-grained picture is justified.

The strain-stress relation results from this energy by the relation $\sigma_{ij} = \partial f/\partial e_{ij}$:

$$\sigma_{xx} = \frac{E}{1-\nu^2}e_{xx} + \frac{\nu}{1-\nu}E_0 e_{yy}, \tag{3a}$$

$$\sigma_{yy} = E_0\left(e_{yy} + \frac{\nu}{1-\nu}e_{xx}\right), \tag{3b}$$

$$\sigma_{xy} = \frac{E_0}{1+\nu}e_{xy}. \tag{3c}$$

3 Stress and strain in perpendicular fracture

We consider a nacre plate with a perpendicular notch crack (much larger than the layer thickness) under a tensile stress in the x direction. We deal with the single edge notched tension (SENT) instead of the three-point bending configuration (see Fig. 3 (a-1)).

3.1 Simplification of the elastic energy

Introducing the Fourier components,

$$u_\alpha(\mathbf{r}) = \frac{1}{(2\pi)^2}\sum_{\mathbf{q}} e^{i\mathbf{q}\cdot\mathbf{r}}u_\alpha(\mathbf{q}),$$

we have

$$\begin{aligned} f_{\mathbf{q}} = &|u_x(\mathbf{q})|^2\left[\frac{E}{2(1-\nu^2)}q_x^2 + \frac{E_0}{4(1+\nu)}q_y^2\right] \\ &+|u_y(\mathbf{q})|^2\left[\frac{E_0}{2}q_y^2 + \frac{E_0}{4(1+\nu)}q_x^2\right] \\ &+u_x(\mathbf{q})u_y(-\mathbf{q})q_x q_y\left[\frac{E_0}{2(1+\nu)} + \frac{\nu E_0}{1-\nu}\right], \end{aligned}$$

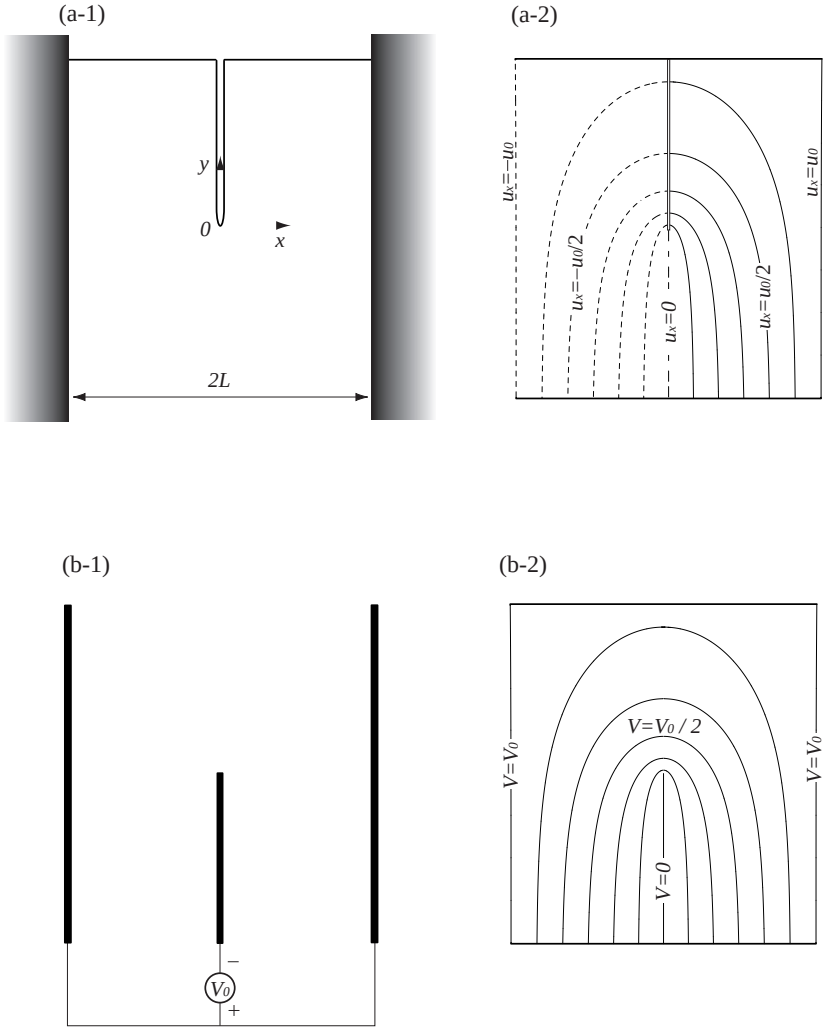

Fig. 3. Analogy between a notch and a variable condenser. (a-1) Notch crack in nacre. (a-2) Corresponding equi-displacement lines. (b-1) Variable Condenser. (b-2) Corresponding equipotential lines. Equi-displacement lines are drawn in the case where ϵ is of the order unity.

where $f_{\mathbf{q}}$ is introduced by

$$F = \int \mathrm{d}\mathbf{r} f = \frac{1}{(2\pi)^2} \sum_{\mathbf{q}} f_{\mathbf{q}}.$$

By minimizing this energy with respect to $u_x(\mathbf{q})$ and $u_y(\mathbf{q})$, we have two linear equations for $u_x(\mathbf{q})$ and $u_y(\mathbf{q})$;

$$\begin{pmatrix} \frac{2}{1-\nu^2} q_x^2 + \frac{\epsilon}{1+\nu} q_y^2 & \epsilon \left(\frac{1}{1+\nu} + \frac{2\nu}{1-\nu} \right) q_x q_y \\ \left(\frac{1}{1+\nu} + \frac{2\nu}{1-\nu} \right) q_x q_y & \frac{1}{1+\nu} q_x^2 + 2 q_y^2 \end{pmatrix} \times \begin{pmatrix} u_x(\mathbf{q}) \\ u_y(\mathbf{q}) \end{pmatrix} = \begin{pmatrix} 0 \\ 0 \end{pmatrix}. \quad (4)$$

To eliminate $u_y(\mathbf{q})$, we use the second equation in equation (4), which is obtained by minimizing F with respect to $u_y(\mathbf{q})$, to get

$$f_{\mathbf{q}} = |u_x(\mathbf{q})|^2 \left[\frac{E}{2(1-\nu^2)} q_x^2 + \frac{E_0}{4(1+\nu)} q_y^2 (1 - \Psi) \right],$$

where

$$\Psi = \frac{1}{4} \left(\frac{1}{1+\nu} + \frac{2\nu}{1-\nu} \right)^2 \frac{q_x^2}{q_x^2 + 2(1+\nu) q_y^2}.$$

By requiring $(u_x(\mathbf{q}), u_y(\mathbf{q})) \neq \mathbf{0}$ in equation (4), we have, via 2×2 matrix determinant equation, two set of solutions. For one of the solution, we have $u_x \sim \epsilon u_y$; u_x is negligible for u_y. This solution is inappropriate under the tensile remote stress σ_∞ in the x direction. The other solution is relevant:

$$q_x^2 \sim -\epsilon q_y^2, \quad (5)$$

$$u_y \sim -\sqrt{\epsilon} u_x. \quad (6)$$

From equation (5), we see that Ψ is the order of ϵ and can be neglected. This implies that the energy is reduced to the following form:

$$f = \frac{E}{2(1-\nu^2)} \left(\frac{\partial u_x}{\partial x} \right)^2 + \frac{E_0}{4(1+\nu)} \left(\frac{\partial u_x}{\partial y} \right)^2. \quad (7)$$

Note that this energy is formally obtained by setting $u_y = 0$ in equation (2).

3.2 Equilibrium strain and stress fields under a remote tensile stress

At equilibrium, the problem reduces to the following Laplace equation obtained by minimizing the volume integral of equation (7) with respect to u_x:

$$\left(\frac{\partial^2}{\partial x^2} + \frac{\partial^2}{\partial \widehat{y}^2}\right) u_x = 0,$$

where

$$\widehat{y} = \sqrt{\frac{2}{\epsilon\,(1-\nu)}}\, y.$$

When the crack tip position is the origin of the axes the appropriate boundary conditions are (see Fig. 3 (a-2))

$$\begin{aligned} &u_x = \pm u_0 \qquad \text{at} \qquad x = \pm L, \\ &u_x = 0 \qquad \text{for} \qquad x = 0,\ y < 0, \\ &\frac{\partial u_x}{\partial x} = 0 \qquad \text{for} \qquad x = 0,\ y > 0. \end{aligned}$$

The last condition corresponds to $\sigma_{xx} = 0$ at the crack surface. This boundary value problem can be solved via conformal transformation, by noting the analogy with a variable condenser (see Fig. 3) [14,15]. The result is (for both cases of $x > 0$ and $x < 0$)

$$u_x = \frac{2u_0}{\pi}\,\mathrm{Im}\left[\log\left(e^{i\pi z/(2L)} + \left(e^{i\pi z/L} - 1\right)^{1/2}\right)\right],$$

with

$$z = x + i\widehat{y}.$$

Here, the branch of $\log z$ with $z = re^{i\theta}$ is such that $\theta = 0$ for real positive z, while that of $z^{1/2}$ is such that $z^{1/2} = i$ for $z = -1$. With this choice of the branches, we have the displacement field shown in Figure 3 (a-2).

The crack shape, $u_x^{(\pm)} \equiv u_x(x = \pm 0)$, is given by (for $y > 0$)

$$u_x^{(\pm)} = \pm\frac{2u_0}{\pi}\arctan\left(\sqrt{e^{\pi\widehat{y}/(2L)} - 1}\right),$$

as shown in Figure 4. In the vicinity of the origin, it reduces to a scaled parabolic form:

$$u_x^{(\pm)} = \pm\frac{2u_0}{\pi}\sqrt{\frac{y}{\xi}},$$

where ξ is defined as

$$\xi = \frac{2\sqrt{\epsilon}}{\pi}L.$$

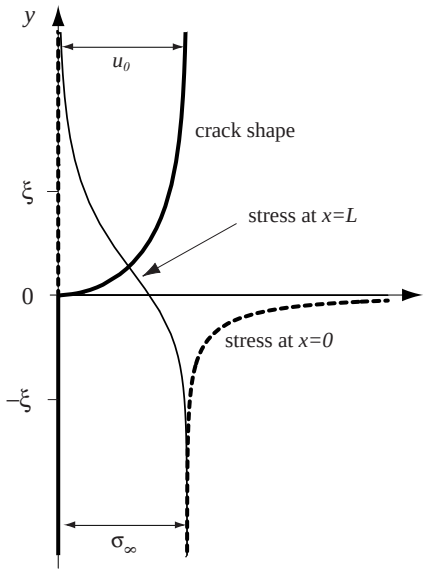

Fig. 4. Crack shape and stress distribution for a perpendicular crack.

Here, we note that ξ is much smaller then the macroscopic scale L.

The stress fields are calculated from equations (3a)-(3c). From equation (6), we can neglect the contributions from u_y field to obtain

$$\sigma_{xx} = \sigma_\infty\,\mathrm{Re}\left[\frac{e^{i\pi z/(2L)}}{\left(e^{i\pi z/L} - 1\right)^{1/2}}\right], \tag{8}$$

where

$$\sigma_\infty = \frac{E}{1-\nu^2}\frac{u_0}{L}. \tag{9}$$

The other components, σ_{yy} and σ_{xy}, are the order of ϵ and $\sqrt{\epsilon}$ (compared with σ_{xx}), respectively, and are neglected in the present approximation.

The stress functions at the crack surface ($x = 0$) and at the fixed edge ($x = L$) are shown in Figure 4. At the crack surface all the stress components are zero as expected. The nonzero stress distribution lies in the region $y < 0$:

$$\sigma_{xx} = \sigma_\infty\frac{e^{-\pi\widehat{y}/(2L)}}{\left(e^{-\pi\widehat{y}/L} - 1\right)^{1/2}}, \tag{10}$$

and the tip singularity is given as (for $y < 0$)

$$\sigma_{xx} = \sigma_\infty\sqrt{\frac{2\xi}{-y}}. \tag{11}$$

At the edge, away from the notch, the stress becomes constant; we can interpret this constant value as the remote tensile stress σ_∞ as already suggested by the notation.

Equation (10) implies that the stress change is rather small for $y \gtrsim \xi$, where $\xi \sim \sqrt{\epsilon}L$ is much smaller than the macroscopic scale but still large compared to the repeat distance d: This justifies our continuum modeling.

Comparing equation (11) with the familiar stress analysis of Irwin for a crack of the size a for the isotropic elastic material,

$$\sigma_{xx} = \sigma_\infty \sqrt{\frac{2a}{-y}},$$

it may be legitimate to call ξ *the effective crack size*. In the case of nacre, this effective crack size is small compared with the macroscopic scale L as announced in [9]. Thus the stress intensity factor (the coefficient of the pressure singularity) is small. We can expect an increase of the material's resistance.

3.3 Fracture toughness and strength

3.3.1 Pure aragonite

For the isotropic pure aragonite, the energy stored in the un-fractured part (away from the crack) is given by

$$f_0 = \frac{1-\nu^2}{2}\frac{\sigma_\infty^2}{E},$$

per unit volume. This results from the classic elastic formulae for an isotropic system under plane strain conditions. Following Griffith's idea of the energy balance, at the moment of failure the energy $f_0 \times 2L$ is equal to twice the surface energy of the aragonite, *i.e.*

$$\left(1-\nu^2\right)\frac{\sigma_\infty^2}{E} L = 2\gamma_{\rm h}.$$

From this we have the failure stress for the pure aragonite,

$$\sigma_{\rm F}^{(0)} = \sqrt{\frac{2E_{\rm h}\gamma_{\rm h}}{\left(1-\nu^2\right)L}}. \tag{12}$$

3.3.2 Nacre

For nacre with a perpendicular fracture, evaluating the energy stored in the un-fractured part by equation (7) as above, we obtain

$$f = \frac{E}{2(1-\nu^2)}\left(\frac{u_0}{L}\right)^2.$$

Following Griffith's idea, the fracture energy is given by $G = f \times 2L$ when $\sigma_\infty = \sigma_{\rm F}$. With the aid of equation (9) this results in

$$G = \left(1-\nu^2\right)\frac{\sigma_{\rm F}^2}{E} L. \tag{13}$$

The stress singularity at the crack tip in equation (11) should be cut off at the distance $\delta(\sim d)$ for a consistent continuum theory where the maximum stress is given by

$$\sigma_1 = \sigma_\infty \sqrt{\frac{2\xi}{\delta}}. \tag{14}$$

This can be interpreted as the stress on the first unbroken aragonite sheet. The fracture tip will advance if and only if $\sigma_1 > \sigma_{\rm YS}$, where $\sigma_{\rm YS}$ is the yield stress of the pure aragonite and is given in equation (1). This in turn gives the failure stress,

$$\sigma_{\rm F} = \sigma_{\rm YS}\sqrt{\frac{\delta}{2\xi}}, \tag{15}$$

From equations (15) and (13), the fracture energy is given by

$$G = \frac{\left(1-\nu^2\right)\delta}{2\sqrt{\epsilon}a_{\rm h}}\gamma_{\rm h}. \tag{16}$$

This is the main result of this paper; it exhibits the enhancement of the fracture energy of nacre compared with that of pure aragonite (see the discussion in Sect. 4).

From equations (15) and (12), we can also see the enhancement of the fracture strength:

$$\sigma_{\rm F} \sim \sqrt{\frac{\delta}{\sqrt{\epsilon}a_{\rm h}}}\sigma_{\rm F}^{(0)}. \tag{17}$$

4 Discussion

Equations (16) and (17) suggest that both the fracture energy and strength are enhanced if $\delta > a_{\rm h}$ (considering the required condition for ϵ, *i.e.* $\epsilon \ll 1$.) Let us examine the orders of magnitude. The cut-off length δ is related to the coarse graining and is of the order of the layer thickness d, *i.e.* $\delta \sim 1\,\mu$m. The size of the Griffith cavity for the pure aragonite is smaller than δ because the aragonite is nearly crystallized, and may be around $a_{\rm h} \sim 50$ nm. The parameter ϵ is estimated at $1/250$, when 95% volume is aragonite and ε is 5000. These estimates give about 1000 and 30 times enhancement of the fracture energy and strength, respectively. The surface energy $\gamma_{\rm h}$ is of order of $1\,{\rm Jm}^{-2}$ (one chemical bond per $(3\,{\rm \AA})^2$). The fracture energy G should then be of the order of 1000 ${\rm Jm}^{-2}$.

The work of fracture is enhanced when nacre is wet. This experimental fact can be also understood from equation (16); in a wet state, $E_{\rm s}$ may become small while $E_{\rm h}$ may stay almost the same to give a decrease in ϵ.

Of course there may be other processes contributing to an increase of toughness: apart from the static effects mentioned in the introduction, we can also have some enhancement from the following two factors. But the contribution discussed by equation (16) should always be present.

A) Plastic flow in the organic component [16,17] and also irreversible slippage of the organic film at the aragonite interface. These questions will require a separate study.

B) Vicoelastic effects in the organic component [18]. If, for the purpose of a simple discussion, we characterize them by a single relaxation time τ, we know

(from previous work on rubbers [18]) the following general features: at distances x (from the fracture tip) smaller than $V\tau$ the elastic moduli stick to their high-frequency value, and the crack shape is the one discussed in our papers. At distances $x > V\tau$ relaxation sets in, and the crack shape will be altered. The overall G will be increased. We propose to discuss these features in a separate publication.

In the case of a parallel crack, the elastic energy in equation (2) is not sufficient. We should include the bending energy of the plates around the crack tip [19–21]. A preliminary analysis (which shall be reported elsewhere) suggests that there is no significant enhancement of toughness in this geometry.

K. Okumura would like to express his sincere gratitude to all the members of de Gennes' group at Collège de France, especially to Achod Aradian, for the warm hospitality during his stay in Paris. He also appreciates informative discussions with Elie Raphaël. and thanks the Japanese Ministry of Education, Science, Sports and Culture for allowing him to stay in Paris.

Appendix A. Derivation of the elastic energy in the thin layer limit

Considering a few layers under the *constant* tensile stress σ_{yy} in the y direction where we neglect the displacement of the hard layer in the y direction while we neglect that of soft layer in the x direction, a macroscopic strain may be expressed as

$$e_{yy}^{(y)} = \frac{d_\mathrm{s}}{d} e_{yy}^{(s)} = \frac{d_\mathrm{s}}{d} \frac{1}{E_\mathrm{s}} \sigma_{yy}, \tag{A.1}$$

$$e_{xx}^{(y)} = e_{xx}^{(\mathrm{h})} = -\frac{\nu}{E_\mathrm{h}} \sigma_{yy}, \tag{A.2}$$

$$e_{zz}^{(y)} = e_{zz}^{(\mathrm{h})} = -\frac{\nu}{E_\mathrm{h}} \sigma_{yy}, \tag{A.3}$$

where $d = d_\mathrm{h} + d_\mathrm{s}$. Here, we have used the relations such as $e_{xx} = [\sigma_{xx} - \nu(\sigma_{yy} + \sigma_{zz})]/E$ for each layer. The superscript (y) indicates that the strain is the one under only σ_{yy}. Under σ_{xx} only, we have

$$e_{xx}^{(x)} = e_{xx}^{(\mathrm{h})} = \frac{1}{E_\mathrm{h}} \sigma_{xx}, \tag{A.4}$$

$$e_{yy}^{(x)} = e_{yy}^{(\mathrm{h})} = -\frac{\nu}{E_\mathrm{h}} \sigma_{xx}, \tag{A.5}$$

$$e_{zz}^{(x)} = e_{zz}^{(\mathrm{h})} = -\frac{\nu}{E_\mathrm{h}} \sigma_{xx}. \tag{A.6}$$

Under σ_{zz} only, we have similar relations for $e_{ii}^{(z)}$ as above. Noting that shearing components do not affect e_{ii}, we have $e_{ii} = e_{ii}^{(x)} + e_{ii}^{(y)} + e_{ii}^{(z)}$ when all the stress components come into play, *i.e.*

$$e_{yy} = \frac{d_\mathrm{s}}{d} \frac{1}{E_\mathrm{s}} \sigma_{yy} - \frac{\nu}{E_\mathrm{h}} (\sigma_{xx} + \sigma_{zz}),$$

$$e_{xx} = \frac{1}{E_\mathrm{h}} \left[\sigma_{xx} - \nu(\sigma_{yy} + \sigma_{zz}) \right],$$

$$e_{zz} = \frac{1}{E_\mathrm{h}} \left[\sigma_{zz} - \nu(\sigma_{yy} + \sigma_{xx}) \right].$$

Considering a few layers under a *constant* shear stress where we neglect the displacement of the hard layer (only the soft layers are deformed), a macroscopic strain is given by

$$e_{xy} = \frac{d_\mathrm{s}}{d} e_{xy}^{(\mathrm{s})} = \frac{d_\mathrm{s}}{d} \frac{1+\nu}{E_\mathrm{s}} \sigma_{xy}, \tag{A.7}$$

where we have used the relation $e_{xy} = \frac{1+\nu}{E} \sigma_{xy}$ for the soft layer. Note here that any other components of the stress tensor do not affect e_{xy}.

In the case of plane strain, we have

$$e_{yy} = \frac{1}{Y_\mathrm{s}} \sigma_{yy} - \frac{1}{Y_\mathrm{h}} \sigma_{xx}, \tag{A.8}$$

$$e_{xx} = \frac{1}{Y_\mathrm{h}} \left(\frac{1-\nu}{\nu} \sigma_{xx} - \sigma_{yy} \right), \tag{A.9}$$

$$e_{xy} = \frac{1+\nu}{Y_\mathrm{s}} \sigma_{xy}, \tag{A.10}$$

with $\sigma_{zz} = \nu(\sigma_{yy} + \sigma_{xx})$. Here,

$$Y_\mathrm{s} = \frac{d}{d_\mathrm{s}} E_\mathrm{s} = \varepsilon \frac{d}{d_\mathrm{s}} E_\mathrm{h},$$

$$Y_\mathrm{h} = \frac{E_\mathrm{h}}{\nu(1+\nu)}.$$

On a macroscopic level, the strains thus introduced and the pressure in these equations can be regarded as continuous variables; the pressures in equations (A.8) to (A.10) are not necessarily constants. Inverting these relations we have

$$\sigma_{xx} = \frac{\nu}{1-\nu} (Y_\mathrm{h} e_{xx} + Y_\mathrm{s} e_{yy}), \tag{A.11}$$

$$\sigma_{yy} = Y_\mathrm{s} (e_{yy} + \frac{\nu}{1-\nu} e_{xx}), \tag{A.12}$$

$$\sigma_{xy} = \frac{Y_\mathrm{s}}{1+\nu} e_{xy}. \tag{A.13}$$

From the formula, $f = \sigma_{ij} e_{ij}/2 = (\sigma_{xx} e_{xx} + \sigma_{yy} e_{yy} + \sigma_{xy} e_{xy} + \sigma_{yx} e_{yx})/2$, the elastic energy is given by

$$f = \frac{\nu Y_\mathrm{h}}{2\,(1-\nu)} e_{xx}^2 + \frac{Y_\mathrm{s}}{2} e_{yy}^2 + \frac{Y_\mathrm{s}}{1+\nu} e_{xy}^2 + \frac{\nu}{1-\nu} Y_\mathrm{s} e_{xx} e_{yy}. \tag{A.14}$$

References

1. T. Kelly, B. Clyne, Phys. Today **52**, 37 (1999).
2. W.J. Clegg, Science **286**, 1097 (1999).
3. R. Naslain, B. Harris (Editors), *Ceramic Matrix Composites: Components, Preparation, Microstructure and Properties* (Elsevier Applied Science, 1989); A.G. Evans, R. Naslain (Editors), *High-temperature Ceramic-matrix Composites* (I, II) (American Ceramic Society, 1994, 1995); F.T. Wallenberger, R. Naslain, E.I. Givargizov (Editors), *Advanced Inorganic Fibres: Processes-Structures-Properties-Applications*, (Chapman & Hall) to be published.
4. S.T. Mileiko, *Metal and Ceramic Based Composites* (Elsevier Science Ltd., 1997); Krishan Kumar Chawla, Krishnan Kumar Chawla, *Composite Materials: Science and Engineering* (Springer-Verlag, 1998); A. Kelly, N.H. Macmillan, *Strong Solids* (Oxford University Press, Oxford, 1986); D. Hull, T.W. Clyne, *An Introduction to Composite Materials* (Cambridge University Press, Cambridge, 1993).
5. J.D. Currey, Proc. R. Soc. Lond. B **196**, 443 (1977).
6. A.P. Jackson, J.F.V. Vincent, R.M. Turner, Proc. R. Soc. Lond. B **234**, 415 (1988).
7. M. Sarikaya, J. Liu, I.A. Aksay, *Biomimetics: Design and Processing of Materials* (AIP Press, New York, 1995) pp. 35-90.
8. M.P. Rao, A.J. Sánchez-Herencia, G.E. Beltz, R.M. McMeeking, F.F. Lange, Science **286**, 102 (1999).
9. P.G. de Gennes, K. Okumura, C. R. Acad. Sci. Paris **1**, Ser. IV, 257 (2000).
10. J.R. Rice, *Fracture: an Advanced Treatise*, edited by H. Liebowitz, Vol. **II** (Academic Press, New York, 1968) pp. 191-311.
11. T.L. Anderson, *Fracture Mechanics-Fundamentals and Applications* (CRC Press, Boca Raton, 1991).
12. B. Lawn, *Fracture of Brittle Solids*, 2nd edition (Cambridge University Press, New York, 1993).
13. S.P. Timoshenko, J.N. Goodier, *Theory of Elasticity*, 3rd edition (McGraw-Hill, 1970).
14. E. Durand, *Électrostatique II* (Masson et C^{ie}, Paris, 1966).
15. P.M. Morse, H. Feshbach, *Methods of Theoretical Physics, II* (McGraw-Hill, New York, 1953).
16. J.S. Langer, H. Nakanishi, Phys. Rev. E **48**, 439 (1993).
17. J.S. Langer, A.E. Lobkovsky, J. Mech. Phys. Solids **46**, 1521 (1998).
18. P.G. de Gennes, Langmuir, **12**, 4497 (1996); *Soft Interfaces* (Cambridge University Press, New York, 1997); C. R. Acad. Paris **307**, Ser. II, 1949 (1988).
19. P.G. de Gennes, Europhys. Lett., **13**, 709 (1990).
20. P.G. de Gennes, in his course at Collège de France (1999).
21. P.G. de Gennes, *The Physics of Liquid Crystal* (Clarendon Press, Oxford, London, 1974).